Complete spherical Bouguer gravity anomalies over Australia

M Kuhn (corresponding author)

Western Australian Centre for Geodesy & The Institute for Geoscience Research, Curtin University of Technology, GPO Box U1987, Perth, WA 6845, Australia

Tel +61 8 9266 7603, Fax + 61 8 9266 2703, M.Kuhn@curtin.edu.au

W E Featherstone

Western Australian Centre for Geodesy & The Institute for Geoscience Research, Curtin University of Technology, GPO Box U1987, Perth, WA 6845, Australia

Tel +61 8 9266 2734, Fax +61 8 9266 2703, W.Featherstone@curtin.edu.au

J F Kirby

Western Australian Centre for Geodesy & The Institute for Geoscience Research, Curtin University of Technology, GPO Box U1987, Perth, WA 6845, Australia

Tel +61 8 9266 7701, Fax +61 8 9266 2703, J.Kirby@curtin.edu.au

ABSTRACT

We have computed complete (or refined) spherical Bouguer gravity anomalies for all 1,095,065 land gravity observations in the June 2007 release of the Australian national gravity database. The spherical Bouguer shell contribution was computed using the supplied ground elevations of the gravity observations. The spherical terrain corrections, residual to each Bouguer shell, were computed on a 9 arc-second grid (~250 m by ~250 m spatial resolution) from a global Newtonian integration using heights from version 2.1 of the GEODATA digital elevation model (DEM) over Australia and the GLOBE and JGP95E global DEMs outside Australia. A constant topographic mass-density of 2670 kg/m^3 was used for both the spherical Bouguer shell and spherical terrain correction terms. The difference between the complete spherical and complete planar Bouguer gravity anomaly exhibits an almost constant bias of about -18.7 mGal over areas with moderate elevation changes, thus verifying the planar model as a reasonable

approximation in these areas. However, the results suggest that in mountainous areas with large elevation changes, the complete spherical Bouguer gravity anomaly should be selected in preference over the less rigorous complete planar counterpart.

Keywords: Spherical Bouguer gravity anomaly, spherical terrain correction, digital elevation models, Australia.

INTRODUCTION

The Bouguer gravity anomaly is frequently used in geophysics to infer geological information from observed gravity (e.g., Ervin 1977; Chapin 1996) and in geodesy to provide boundary values on the geoid, which have been reduced by the gravitational attraction effect of all masses above the geoid (e.g., Heiskanen & Moritz 1967; Vaníček *et al.* 2004). Central to both the geophysical and geodetic views is the requirement to algebraically consider the gravitational effects of the topographic masses. While the general definition of the Bouguer gravity anomaly (either geophysical or geodetic) does not contain any approximation, the gravitational effect of the topographic masses is frequently approximated, thus leading to different variants of the Bouguer gravity anomaly (e.g., Heiskanen & Moritz 1967; Ervin 1977; Chapin 1996; Vaníček *et al.* 2001; 2004).

The simple planar Bouguer gravity anomaly only considers the gravitational effect of an infinitely planar plate (Bouguer plate or slab) whose thickness is equal to the elevation of the gravity observation, whereas the complete (or refined) planar Bouguer gravity anomaly also considers the gravitational effect of the terrain, residual to the Bouguer plate (planar terrain correction). The planar model, however, only provides a crude approximation of reality, which is not the case for a spherical model providing an approximation closer to reality (e.g., Karl 1971; Qureshi 1976; Ervin 1977; Chapin 1996; LaFehr 1998; Nowell 1999; Smith *et al.* 2001; Vaníček *et al.* 2001; 2004). In analogy to the planar case, the simple spherical Bouguer gravity anomaly only considers the gravitational effect of a spherical Bouguer shell, and the complete spherical Bouguer gravity anomaly additionally considers the gravitational effect of the topography residual to the spherical shell (spherical terrain correction). In terms of the computational

effort required, one disadvantage of the spherical model is that terrain corrections have to be computed over the global topography, whereas they need only be computed over a smaller area in the planar case.

In the past, the planar approximation has often been used to compute Bouguer gravity anomalies (both simple and complete), even though extra corrections that account for the more realistic spherical shape of the Earth (e.g., Bullard B correction) were introduced a long time ago (see the references in Takin & Talwani 1966; LaFehr 1991b and Nowell 1999 and the discussions in Hensel 1992 and LaFehr 1992). If these spherical terms are not accounted for, significant distortions may be introduced in the corresponding Bouguer gravity anomalies (e.g., LaFehr 1991a; 1991b; 1992; Talwani 1998). One possible reason for the frequent use of the simple planar Bouguer gravity anomaly is the extremely simple computation procedure to obtain the gravitational effect of the Bouguer plate, thus requiring minimal computational power. Moreover, the planar terrain correction only has to consider the topography surrounding the computation point (e.g., up to Hayford zone O, 166.7 km). Finally, fast Fourier transform (FFT) techniques can be employed to compute a whole grid of planar terrain corrections very efficiently (e.g., Parker 1972; Forsberg 1985; Sideris 1985; Li & Sideris 1994; Parker 1995; 1996; Kirby & Featherstone 1999, 2002; Featherstone & Kirby 2002).

On the other hand, the determination of spherical terrain corrections, hence complete spherical Bouguer gravity anomalies, cannot be adapted to FFT techniques as yet, and also require the global topography to be taken into account. Therefore, the large computational power required, coupled with the need for a global digital elevation model (DEM), probably account for the major restrictions against the widespread computation and use of the complete spherical Bouguer gravity anomaly.

In this paper, we demonstrate that this is no longer a restriction because of the power of reasonably low-cost computers and the free availability of global high-resolution DEMs. We computed spherical terrain corrections on a 9-arc-second by 9-arc-second grid (~250 m) over all Australia, which were then used to derive complete spherical Bouguer gravity anomalies for all land gravity stations in the 2007 release of Geoscience Australia's (GA's) gravity database (Murray 1997). Like the planar terrain corrections and complete planar Bouguer gravity anomalies (Kirby & Featherstone

1999; 2002; Featherstone & Kirby 2002), the spherical terrain corrections and the complete spherical Bouguer gravity anomalies will be supplied to GA for evaluation and possible future inclusion in the national gravity database.

THEORY AND METHODOLOGY

Bouguer gravity anomaly

There are two conceptually different views of the Bouguer gravity anomaly (e.g., Li & Götze 2001; Hackney & Featherstone 2003; Vaníček *et al.* 2004): (1) In geophysics (e.g., Ervin, 1977; Chapin, 1996), the Bouguer gravity anomaly is defined at the location of the gravity observation and the Bouguer reduction aims to model and remove all "non-geological effects". This also requires upward continuation of normal gravity from the surface of the reference ellipsoid to the location of the gravity observation via the free-air correction (or reduction). (2) In geodesy (e.g., Heiskanen & Moritz 1967; Vaníček *et al.* 2004), the Bouguer gravity anomaly is required on the geoid where the gravitational attraction of the topographic masses (including all geologically interesting mass variations) should be removed completely. This also requires downward continuation of gravity from the observation location to the geoid (e.g., Vaníček *et al.* 2001; 2004). Although there is this conceptual difference, the formulae, practical determination and numerical values of the geophysical and geodetic Bouguer gravity anomalies are identical if the same term to upward continue normal gravity is used.

The Bouguer gravity anomaly at the gravity observation is given by

$$\Delta g_B = g_P - \delta g_{TOP} + \delta g_{AC} + \delta g_{FC} - \gamma_0 \qquad (1)$$

where g_P is the observed gravity at point *P* (e.g., on the Earth's surface), δg_{TOP} and δg_{AC} are the gravitational attraction of the topographic masses (complete Bouguer correction or topographic reduction) and atmospheric masses (atmospheric correction), respectively, δg_{FC} is the free-air correction and γ_0 is normal gravity on the surface of the reference ellipsoid. In Eq. (1), the combined effect of δg_{TOP} and δg_{AC} removes the gravitational attraction of all masses outside the geoid.

The Bouguer gravity anomaly defined by Eq. (1) is exact in the sense that it does not use any approximations about the shape of and mass distribution in the topography. However, different approximations for δg_{TOP} have been introduced, resulting in the simple and complete planar Bouguer gravity anomalies (Δg_{SPB} and Δg_{CPB}) and the simple and complete spherical Bouguer gravity anomalies (Δg_{SSB} and Δg_{CSB}).

The simple *planar* Bouguer gravity anomaly Δg_{SPB} uses the approximation $\delta g_{TOP} \approx \delta g_{BP}$, which is the gravitational effect of the infinitely lateral Bouguer plate of constant thickness H_P corresponding to the height (above the geoid) of the gravity observation. The gravitational effect of the Bouguer plate is given by $\delta g_{BP} = 2\pi G\rho H_P$, where ρ is the (constant) mass-density of the Bouguer plate and G is the universal gravitational constant.

$$\Delta g_{SPB} = g_P - \delta g_{BP} + \delta g_{AC} + \delta g_{FC} - \gamma_0 \tag{2a}$$

The planar terrain correction δg_{PTC} is added to this to give the complete planar Bouguer gravity anomaly Δg_{CPB}, thus accounting – in an approximate way – for the gravitational effect of the topography residual to the Bouguer plate.

$$\Delta g_{CPB} = \Delta g_{SPB} + \delta g_{PTC} \tag{2b}$$

The simple *spherical* Bouguer gravity anomaly Δg_{SSB} uses the approximation $\delta g_{TOP} \approx \delta g_{BS}$, which is the gravitational effect of the Bouguer shell of constant thickness H_P. The gravitational attraction of the Bouguer shell is $\delta g_{BP} = 4\pi G\rho H_P$, being twice as large as that of the Bouguer plate

$$\Delta g_{SSB} = g_P - \delta g_{BS} + \delta g_{AC} + \delta g_{FC} - \gamma_0 \tag{2c}$$

The (global) spherical terrain correction δg_{STC} is added to give the complete spherical Bouguer gravity anomaly Δg_{CSB}, thus accounting for the global topography residual to the spherical shell.

$$\Delta g_{CSB} = \Delta g_{SSB} + \delta g_{STC} \tag{2d}$$

The spherical terrain correction is much larger (takes the global terrain into account) than the planar terrain correction, thus countering the larger Bouguer shell term (see the discussion later).

Gravimetric terrain corrections

For both the complete planar and complete spherical Bouguer gravity anomalies, the corresponding terrain corrections must be determined. With respect to all other reductions in Eq. (1), this is the most computationally intensive task. Both the planar and spherical terrain corrections represent the gravitational attraction of the residual topography (with respect to the Bouguer plate or shell). Their contributions to the topographic reductions are indirectly defined through $\delta g_{TOP}^{planar} = \delta g_{BP} - \delta g_{PTC}$ and $\delta g_{TOP}^{spherical} = \delta g_{BS} - \delta g_{STC}$, given through Eqs. (2b) and (2d), respectively.

While the planar terrain correction δg_{PTC} is always positive for stations on land (e.g., Hammer 1939) this is not the case for the spherical terrain correction, where the additional masses above the Bouguer shell count positive/negative when located above/below the local horizon of the gravity observation (cf. Figure 1). Therefore, especially for low elevation gravity observations, the spherical terrain correction is generally negative (cf. Nowell 1999), as will be shown in the next section. [Note that terrain corrections can also be negative for airborne or marine gravity observations.]

[Figure 1]

We determined the spherical terrain corrections through the application of Newton's integral by discretised numerical integration based on spherical volume elements defined by the compartments of a DEM in geodetic coordinates. The gravitational attraction of the corresponding masses is obtained through the superposition of the gravitational attraction of a series of spherical volume elements (tesseroids) over the whole Earth (Kuhn, 2003). The "innermost-zone" effect (i.e., terrain undulations around the computation point that have a smaller spatial resolution then that of the DEM used) has been neglected in this approach (cf. Leaman, 1998). As such, the spherical terrain corrections omit near-meter effects, as was the case for the planar terrain corrections com-

puted by Kirby & Featherstone (1999, 2002). Leaman (1998) shows that the near-meter effect can reach almost 0.1 mGal in only moderately undulating terrain, thus has to be accounted for in very precise gravity surveys. However, these effects are of less importance for this study as they are practically the same for planar and spherical terrain corrections, thus will cancel when both models are compared to each other (cf. Figure 5).

Free-air correction

Here we follow the common approach where the free-air correction δg_{FC} is approximated by the vertical gradient of normal gravity (e.g., Heiskanen & Moritz 1967). However, we do not use the linear approximation of 0.3086 mGal/m, but a second-order approximation that accounts for both a change of the gravity gradient with height and with geodetic latitude (ϕ) (e.g., Featherstone 1995). The second-order approximation of the free-air reduction is

$$\delta g_{FAC} = \frac{2\gamma_0}{a}(1 + f + m - 2f\sin^2\phi)H_P - \frac{3\gamma_0}{a^2}{H_P}^2 \qquad (3)$$

where H_P is the height of the gravity observation at *P* above the geoid, *f* is the geometrical flattening of the reference ellipsoid, *m* is the geodetic parameter, which is the ratio of gravitational and centrifugal forces at the equator, and *a* is the semi-major axis length (equatorial radius) of the reference ellipsoid used (see Table 1). Over Australia with an average height of 272 m (min: -16 m, max: 2228 m, cf. Figure 3), the average difference between the free-air correction using Eq. (3) and the linear approximation is 0.017 mGal with a maximum value of 0.318 mGal. Therefore, the use of Eq. (3) in preference to the linear approximation of the free-air correction is important for precise gravity surveys at elevation.

Atmospheric correction

In contrast to the frequently used definition of the Bouguer gravity anomaly (e.g. Ervin 1977; Chapin 1996), we now include the atmospheric correction δg_{AC}, which is theoretically necessary because the reference ellipsoid includes the gravitational effect of the atmospheric masses, which is the case for GRS80 (Moritz 1980), and thus has to be re-

moved. The atmospheric correction is modelled by a second-order polynomial fit to the values in IAG (1971) (cf. Featherstone & Dentith 1997).

$$\delta g_{ATC} = 0.871 - 1.0298 \times 10^{-4} H_P + 5.3105 \times 10^{-9} {H_P}^2 \quad \text{[mGal]} \tag{4}$$

Over the Australian elevation range between -16 m and 2228 m, the range of the atmospheric correction over Australia is between 0.871 mGal and 0.668 mGal.

Normal gravity (latitude correction)

We use the more exact Somigliana-Pizzetti closed formula (e.g., Heiskanen and Moritz 1967, Eq. 2-78) instead of the Chebyshev approximations often used in geophysics (cf. Chapin 1996; Li & Götze, 2001) to compute normal gravity γ_0 (also called the latitude correction in geophysics). The Somigliana-Pizzetti formula, given here in a numerically more convenient form (cf. Moritz 1980), is

$$\gamma_0 = \gamma_e \frac{1 + k \sin^2 \phi}{\sqrt{1 - e^2 \sin^2 \phi}} \tag{5}$$

where k is the normal gravity constant, γ_e is normal gravity acceleration at the equator, e^2 is the square of the first numerical eccentricity of the reference ellipsoid, and ϕ is the geodetic latitude. If desired, a higher accuracy formula for normal gravity is given in Ardalan & Grafarend (2001), but γ_0 derived by Eq. (4) is already one order of magnitude more accurate than the accuracy of modern gravimeters.

For geodetic applications, the GRS80 reference ellipsoid is usually used (e.g., Hackney & Featherstone, 2003), whereas the WGS84 reference ellipsoid is commonly used in geophysical applications (e.g., Fairhead et al. 2003). Differences in the normal gravity value using either the GRS80 or WGS84 reference ellipsoid are almost constant throughout Australia. The magnitude of their difference is 0.143 mGal, but their variation is less than 1 μGal over the latitude range between 10°S and 45°S.

Numerical values of the parameters used

Table 1 lists numerical values of the parameters needed in the above equations for GRS80 (Moritz, 1980), WGS84 (NIMA, 2000) and the best-available estimate of the

universal gravitational constant from the Committee on Data for Science and Technology's (CODATA's) 2006 release of the fundamental physical constants. It is worth pointing out that the free-air gravity anomalies supplied in the GA database are also computed using a second-order free-air correction, but for the now-outdated GRS67 reference ellipsoid (IAG, 1971). Since the Geocentric Datum of Australia 1994 (GDA94) uses the GRS80 ellipsoid, it is logical to use this international standard to achieve currency and consistency. As such, all gravity anomalies recomputed here use the GRS80 ellipsoid parameters in Table 1.

[Table 1]

DATA USED

The Australian national gravity database

In this study, we used all 1,095,065 land gravity observations in the Australian national gravity database (Murray 1997), which are now freely available via a web-based delivery system (http://www.geoscience.gov.au/gadds), though subject to licence conditions. All land gravity observations were extracted from the database in June 2007 (hereafter called the 2007 release) and their spatial distribution is illustrated in Figure 2. The gravity datum is ISOGal84 (Wellman & Murray 1985), which is tied to the global international gravity standardisation network, IGSN71 (Morelli *et al.* 1974).

[Figure 2]

GEODATA, GLOBE and JGP95E DEMs

The topographic masses over Australia were modelled from the 9-arc-second by 9-arc-second (~250 m spatial resolution) GEODATA (version 2.1) DEM (Hutchinson, 2001), which is now freely available at http://www.ga.gov.au/products/digidat/dem.htm (Figure 3). The GEODATA DEM was extended to 100ºE to 165ºE and 0ºS to 55ºS, where areas around Australia were filled in by the 30-arc-second by 30-arc-second (~1 km spatial resolution) GLOBE v1 global DEM (Hastings & Dunbar 1998).

While the 9-arc-second GEODATA DEM provides sufficient information to compute planar terrain corrections (Kirby & Featherstone 1999; 2002), spherical terrain corrections require information about the global topographic mass distribution. These were modelled outside the area specified above from the 5-arc-minute by 5-arc-minute (~10 km by spatial resolution) JGP95E global DEM (Lemoine *et al.* 1998, chapter 2), which classifies the terrain into six different types: (1) dry land below mean sea level, (2) lake, (3) oceanic ice shelf, (4) ocean, (5) glacier ice, (6) dry land above mean sea level. These different mass distributions were converted into equivalent rock heights using mass-balance formulae in spherical approximation (e.g., Rummel *et al.*, 1988; Kuhn & Seitz, 2005) for a constant topographic mass-density of 2,670 kg/m^3. Effectively, this replaces the ocean water masses by a smaller thickness of rock masses. Thus, the ocean is effectively replaced by rock with smaller depth values (with respect to the ocean surface) than the original bathymetry due to the larger density (2,670 kg/m^3 for rock and 1,030 kg/m^3 for seawater).

So as to profit from increased spatial resolution, JGP95E was replaced by the 9-arc-second GEODATA DEM over Australia (filled in with the GLOBE DEM, see above), arithmetically averaged to a 5-arc-min grid, which ensures that there is no difference in mass distribution caused by the use of DEMs with different resolutions. Furthermore, the combined GEODATA/GLOBE/JGP95E DEM has been generalised (by arithmetical averaging) to four coarser resolutions as specified in Table 2. This is permitted because the gravitation attraction decreases with distance-squared, so lower resolutions can be used in remote regions to accelerate computations while not compromising accuracy.

The coarser resolutions and corresponding areas were chosen empirically so that the corresponding approximation error (with respect to the finer resolution) always remained below 1 μGal for the spherical terrain correction (e.g. Kuhn, 2003). Table 2 also shows the spatial extension over which a given DEM resolution has been applied to determine the global spherical terrain corrections.

[Table 2] & [Figure 3]

RESULTS

Here we focus on the spherical Bouguer gravity anomaly (simple and complete) and the spherical terrain correction, but provide comparisons with planar Bouguer gravity anomalies computed by Kirby & Featherstone (2002). These four approximations of the Bouguer gravity anomaly are determined according Eqs. (2a) to (2d), where the free-air correction, atmospheric correction and normal gravity are determined according Eqs. (3), (4) and (5), respectively. All numerical results for the Bouguer gravity anomalies and terrain corrections are presented in Figures 4 and 5 and are based on the constant topographic mass-density of 2670 kg/m^3 and the numerical values of the parameters in Table 1.

For display purposes, the Bouguer gravity anomalies, terrain corrections in Figure 4 and differences in Figure 5 at the locations of the gravity observations have been interpolated onto a 15-arc-min by 15-arc-min (~25 km spatial resolution) grid using tensioned splines with a tension factor of T=0.25 (Smith & Wessel, 1990). Furthermore, Figures 2 to 5 have been produced using the Generic Mapping Tools software (Wessel & Smith, 1998; http://gmt.soest.hawaii.edu/). In Figures 4 and 5, no data are displayed outside the area defined by the GEODATA DEM.

Planar Bouguer gravity anomalies

The simple planar Bouguer gravity anomaly in Figure 4a was calculated according to Eq (2a), where the height H_P is the ground height of the observation location provided in the June 2007 GA database. The complete planar Bouguer gravity anomaly was derived from the simple planar Bouguer gravity anomaly by *adding* the planar terrain correction (Figure 4b), which has been interpolated (bi-cubic) at each gravity observation location from the 9-arc-second grid of planar terrain corrections given by Kirby and Feathestone (2002). The planar terrain corrections and the complete planar Bouguer gravity anomalies are illustrated in Figures 4b and 4c, respectively.

Spherical Bouguer gravity anomalies

The simple spherical Bouguer gravity anomaly (Figure 4d) was computed according Eq. (2c) where the computational effort to determine the simple planar and spherical effects is exactly the same.

The 9-arc-second DEM was used to determine the gravitational effect of the residual (to each Bouguer shell) topographical masses in the vicinity of the computation point out to 15 by 15 arc-minutes (approximately out to Hayford zone L). The contribution to the spherical terrain correction from the remaining distant global residual terrain masses was computed from the combination of the GEODATA, GLOBE and JGP95E DEMs generalised to coarser resolutions for the more distant topographic masses around the computation point (cf. Table 2). A total of 111,402,348 terrain corrections at the nodes of the 9-arc-second DEM were computed over all Australian landmasses, which took about two months on a Sun UNIX workstation with two parallel 1 GHz processors and 16 Gb of core RAM.

Figure 4e shows that the spherical terrain correction is negative (unlike the always-positive planar terrain correction on land) in low elevation areas on land. These spherical terrain corrections were algebraically added to the simple spherical Bouguer gravity anomalies to give the complete spherical Bouguer gravity anomalies (Eq. 2d). As for the planar terrain correction, the spherical terrain correction was bi-cubically interpolated from the 9-arc-second grid of spherical terrain corrections to each gravity observation location. The spherical terrain corrections and the complete spherical Bouguer gravity anomalies are illustrated in Figures 4e and 4f, respectively.

[Figure 4]

DISCUSSION

First, it is informative to look at the descriptive statistics (minimum, maximum, mean, standard deviation and RMS) of the different approximations of the Bouguer gravity anomaly and the terrain corrections (Table 3). The statistics of the planar and spherical

terrain corrections are also given in Table 3 for both the whole 9-arc-second grid and when interpolated to the gravity observation locations.

[Table 3]

From the mean values in Table 3, the various approximations of the Bouguer gravity anomalies are all largely negative (cf. Figures 4a, 4c, 4d and 4f). This is a well-known characteristic of Bouguer gravity anomalies on land, which shows that the topographic masses are generally isostatically compensated by mass anomalies in the lithosphere, at least at very long (> thousands of km) wavelengths (e.g., Watts, 2001). From the standard deviations in Table 3, despite the fact that Bouguer gravity anomalies are supposed to be smoother than free-air gravity anomalies (cf. Goos et al., 2003), the standard deviation of the latter is smaller. However, this is not because the Bouguer gravity anomalies are "rougher", but the higher standard deviations are due to the large negative values for most of the anomalies (Table 3).

Comparing the simple planar and spherical Bouguer gravity anomalies (cf. Figures 4a and 4d), the spatial structure appears identical, but the magnitudes are different. The range (maximum minus minimum) is larger for the simple spherical Bouguer gravity anomaly, which is caused largely by the gravitational attraction of the Bouguer shell being twice as large as that of the Bouguer plate. Similarly, comparing Figures 4b and 4e, the planar and spherical terrain corrections exhibit similar spatial characteristics, but the magnitudes are also different. While most of the planar terrain corrections are small over Australia (over 92% of values are less than 0.5 mGal), the spherical terrain corrections can reach magnitudes of over 200 mGal.

Furthermore, as illustrated in Figure 4e, the spherical terrain correction can be negative, which is evident in most low-lying areas (e.g. Lake Eyre and the Murray-Darling river basin). This is because a considerable part of the global terrain masses are below the local horizon of the computation point but above the spherical shell, thus contributing negatively to the spherical terrain correction (also see Figure 1).

The large difference in absolute magnitude between the planar and spherical terrain corrections is because the spherical terrain correction takes the gravitational attrac-

tion of the global topography into account. This is contrary to the behaviour of the planar terrain correction, where only terrain masses in the close proximity contribute to the planar terrain correction and masses further away (e.g., beyond Hayford zone O) can be neglected. As such, the planar terrain correction is generally small (cf. Figure 4) and usually only has to be accounted for in mountainous areas (e.g. Hammer 1939). This is in contrast to the spherical terrain correction, where most of the contribution comes from the global terrain masses, rather than the masses in the close proximity to the computation point (e.g., compare the statistical values for the planar and spherical terrain corrections in Table 2).

Finally, comparing the complete planar and complete spherical Bouguer gravity anomalies (cf. Figures 4c and 4f) shows that they are very similar both in spatial structure and magnitude (cf. Table 3). Therefore, the different magnitudes between them and the planar and spherical terrain corrections largely compensate one another. Figure 5 shows the difference between the complete planar and complete spherical Bouguer gravity anomalies, which exhibits an almost-constant difference over large areas with minor spatial variations of a few mGal. Only over mountainous areas the spatial variations of the differences reach magnitudes of > 10 mGal.

The average difference of -18.66 mGal (Table 3) approximately corresponds to the far-zone effect of the topographic reduction in the spherical approximation. This represents the gravitational effect of the global topographic masses, thus excluding masses in the localised area that have been considered by the planar terrain correction. The NW to SE trend visible in Figure 5 is the result of the relative location of the computation points with respect to the global topographic masses (e.g., differences are more negative in the NW due to the closer proximity to the Himalayas, which cause the spherical terrain corrections to be more negative).

Over areas with moderate elevation changes, this result bodes well for the interpretation of (complete) planar Bouguer gravity anomalies in that, disregarding the bias, they appear to be generally good approximations of their theoretically more rigorous spherical counterparts. For instance, they might be sufficient for geological interpretations, so long as the focus remains localised. In these areas, it may suffice to use only the simple planar Bouguer gravity anomalies, especially as the planar terrain corrections

are mostly less than 0.5 mGal in these parts of Australia. Only over mountainous areas may local geological interpretation be distorted when the complete planar Bouguer gravity anomaly is used in preference over the more rigorous complete spherical Bouguer gravity anomaly.

[Figure 4]

CONCLUDING REMARKS

We have shown that, with reasonably modest modern computer power and the free availability of global and regional DEMs, spherical terrain corrections and thus complete spherical Bouguer gravity anomalies can be computed on a very dense grid over continental-size areas. However, should this computational effort seem unattractive, we have also shown that planar Bouguer gravity anomalies turn out to be a very good approximation, at least over large areas of Australia with only moderate elevation changes.

In these areas, the difference between the complete planar and complete spherical Bouguer gravity anomalies manifests as an almost constant bias (over 92% of differences are in a band of ± 2.5 mGal around the average of -18.660 mGal), suggesting that the choice of either approach is of minor importance for most applications in geophysical exploration and geodesy. Only in areas with large elevation changes does the choice of the type of Bouguer gravity anomaly become more critical (cf. Flis et al. 1998). In these cases, we recommend the use of the more rigorous complete spherical Bouguer gravity anomaly for geodetic applications, as the aim is to completely remove the global topography. For geophysical applications with the aim of modelling known mass distributions only rather close to the computation point (e.g. up to a few hundred kilometres), it seems the planar model or a spherical model with limited extension around the computation point are more appropriate, thus the additional computational effort to compute the complete spherical Bouguer anomaly may not be justified.

The complete spherical terrain corrections and Bouguer gravity anomalies will be supplied to Geoscience Australia for further evaluation and possible subsequent distribution to users via the Australian national gravity database.

ACKNOWLEDGMENTS

We would like to thank Geoscience Australia for providing the GEODATA (version 2.1) DEM and gravity data over Australia. Grateful thanks go to the reviewers Prof Derek Fairhead and Ray Tracey for their valuable comments. This is TIGeR publication number xxx.

REFERENCES

ARDALAN A. A. & GRAFAREND E. W. 2001. Somigliana-Pizzetti gravity: the international gravity formula accurate to the sub-nanogal level. *Journal of Geodesy*, **75**(7), 424–437, doi: 10.1007/PL00004005

CHAPIN D. A. 1996. The theory of the Bouguer gravity anomaly: A tutorial. *The Leading Edge*, **15**, 361–363.

ERVIN C. P. 1977. Theory of the Bouguer anomaly. *Geophysics*, **42**(7), 1468.

FAIRHEAD J.D., GREEN C.M. & BLITZKOW D. 2003 The use of GPS in gravity surveys, *The Leading Edge* **22**(10), 954-959, doi: 10.1190/1.1623636.

FEATHERSTONE W. E. 1995. On the use of Australian Geodetic Datums in gravity field determination. *Geomatics Research Australasia*, **62**, 17-36.

FEATHERSTONE W. E. & DENTITH M. C. 1997. A geodetic approach to gravity reduction for geophysics. *Computers and Geosciences*, **23**(10), 1063–1070, doi: 10.1016/S0098-3004(97)00092-7

FEATHERSTONE W. E. & KIRBY J. F. 2002. New high-resolution grid of gravimetric terrain corrections over Australia. *Australian Journal of Earth Sciences* **49**(5), 733-734, doi: 10.1046/j.1440-0952.2002.00952.x.

FLIS M. F., BUTT A. L. & HAWKE P. J. 1998. Mapping the range front with gravity—are the corrections up to it? *Exploration Geophysics*, **29**(4) 378–383

FORSBERG R. 1985. Gravity field terrain effect computations by FFT. *Bulletin Géodésique*, **59**(4), 342–360.

GOOS J. M., FEATHERSTONE W.E., KIRBY J. F., HOLMES S.A. 2003. Experiments with two different approaches to gridding terrestrial gravity anomalies and their effect on regional geoid computation. *Survey Review* 37, 92-112.

HACKNEY R .I. & FEATHERSTONE W. E. (2003) Geodetic versus geophysical perspectives of the 'gravity anomaly', *Geophysical Journal International* **154**(1): 35-43, doi: 10.1046/j.1365-246X.2003.01941.x [Errata in *Geophysical Journal International* **154**(2): 596, doi: 10.1046/j.1365-246X.2003.02058.x and *Geophysical Journal International* **167**(2): 585-585, doi: 10.1111/j.1365-246X.2006.03035.x].

HAMMER S. 1939. Terrain corrections for gravimeter stations. *Geophysics*, **4**(3), 184–194, doi:10.1190/1.1440495

HASTINGS D. A. & DUNBAR P. K. 1998. Development and assessment of the global land one-km base elevation digital elevation model (GLOBE). *ISPRS Arch*, **32**, 218–221. http://www.ngdc.noaa.gov/mgg/topo/globe.html.

HEISKANEN W. A. & MORITZ H. 1967. *Physical Geodesy*. Freeman, San Francisco.

HENSEL E. G. 1992. Discussion on: "An exact solution for the gravity curvature (Bullard B) correction" by T. R. LaFehr. *Geophysics*, **57**, 1093–1094.

HUTCHINSON M. F. (ed) 2001. GEODATA 9 second DEM (version 2): Data users guide, Geoscience Australia, Canberra, 46pp.

IAG 1971. Geodetic Reference System 1967. International Association of Geodesy, *Special Publication no. 3 of Bulletin Géodésiqu*e, 116pp

KARL J. H. 1971. The Bouguer correction for the spherical Earth. *Geophysics*, **36**(4), 761–762, doi:10.1190/1.1440211

KIRBY J. F. & FEATHERSTONE W.E. 1999. Terrain correcting Australian gravity observations using the national digital elevation model and the fast Fourier transform. *Australian Journal of Earth Sciences*, **46**(4), 555–562, doi: 10.1046/j.1440-0952.1999.00731.x

KIRBY J. F. & FEATHERSTONE W.E. 2002. High-resolution grids of gravimetric terrain correction and complete Bouguer corrections over Australia. *Exploration Geophysics*, **33**(4), 161-165, doi:10.1071/EG02161

KUHN M. 2003. Geoid Determination with Density Hypotheses from Isostatic Models and Geological Information. *Journal of Geodesy*, 77: 50-65, doi:10.1007/s00190-002-0297-y.

KUHN M. & SEITZ K. (2005) Evaluation of Newton's integral in space and frequency domain. In: Sansò F (ed) *A Window on the Future of Geodesy*. Springer, Berlin Heidelberg NewYork, pp 386-391, doi: 10.1007/3-540-27432-4_66.

LAFEHR T. R. 1991a. Standardisation in gravity reduction. *Geophysics*, **56**(8), 1170–1178, doi 10.1190/1.1443137

LAFEHR T. R. 1991b. An exact solution for the gravity curvature (Bullard B) correction. *Geophysics*, **56**(8), 1179–1184, doi:10.1190/1.1443138

LAFEHR T. R. 1992. Discussion on: "An exact solution for the gravity curvature (Bullard B) correction" by T. R. LaFehr. *Geophysics*, **57**, 1094.

LAFEHR T. R. 1998. On Talawani's "Errors in the total Bouguer reduction". *Geophysics*, **63**(4), 1131-1136, doi:10.1190/1.1444413

LEAMAN D. E. 1998. The gravity terrain correction – practical considerations. *Exploration Geophysics*, **29**(4), 476–471, doi:10.1071/EG998467

LEMOINE F. G., KENYON S. C., FACTOR J. K., TRIMMER R. G., PAVLIS N. K., CHINN D. S., COX C. M., KLOSKO S. M., LUTHCKE S. B., TORRENCE M. H., WANG Y. M., WILLIAMSON R. G., PAVLIS E. C., RAPP R. H., OLSON T. R. 1998. *The development of the joint NASA GSFC and the National Imagery and Mapping Agency (NIMA) geopotential model EGM96*, TP-1998-206861, National Aeronautics and Space Administration, Greenbelt, USA, 575 pp.

LI X. & GÖTZE H.-J. 2001. Ellipsoid, geoid, gravity, geodesy and geophysics. *Geophysics*, **66**(6), 1660–1668, doi:10.1190/1.1487109

LI Y. C. & SIDERIS M. G. 1994. Improved gravimetric terrain corrections. *Geophysical Journal International*, **119**(3), 740–752, doi:10.1111/j.1365-246X.1994.tb04013.x

MORELLI, C., GANTER, C., HANKASALO, T., MCCONNELL, R.K., TANNER, J.B., SZABO, B., UOTILA, U. & WHALEN, C.T. 1974, The International Gravity Standardization Net 1971, Special Publication 4, International Association of Geodesy, Paris.

MORITZ H. 1980. Geodetic reference system 1980. *Bulletin Géodésique*, **54**(4) 395–405, doi: 10.1007/BF02521480

MURRAY A. S. 1997. The Australian national gravity database. *AGSO Journal of Australian Geology and Geophysics*, **17**(1), 145–155.

NIMA 2000. Department of Defence World Geodetic System 1984. Technical report NIMA TR8350.2, pp. 175 (http://earth-info.nga.mil/GandG/publications/tr8350.2/wgs84fin.pdf).

NOWELL D. A. G. 1999. Gravity terrain corrections — an overview. *Journal of Applied Geophysics*, **42**(2) 117–134, doi: 10.1016/S0926-9851(99)00028-2

PARKER R. L. 1972. The Rapid Calculation of Potential Anomalies. *Geophys. J. R. astr. Soc.* **31**, 447-455.

PARKER R. L. 1995. Improved Fourier terrain correction: Part I. *Geophysics*, **60**(5), 1007–1017, doi: 10.1016/0148-9062(96)80035-0

PARKER R. L. 1996. Improved Fourier terrain correction: Part II. *Geophysics*, **61**(2), 365–372, doi: 10.1190/1.1443965

QUERSHI I. R. 1976. Two-dimensionality on a spherical Earth – a problem in gravity reductions. *Pure and Applied Geophysics*, **114**(1), 91–93, doi: 10.1007/BF00875494

RUMMEL R., RAPP H. R., SUENKEL H. 1988. Comparison of global topographic/isostatic models to the Earth's observed gravity field, Rep 388, Department Geodesic Science and Survey, Ohio State University, Columbus, 33 pp

SIDERIS M. G. 1985. A fast Fourier transform method of computing terrain corrections. *manuscripta geodaetica*, **10**(1), 66–73.

SMITH D. A., ROBERTSON D. S. & MILBERT D. G. 2001. Gravitational attraction of local crustal masses in spherical coordinates. *Journal of Geodesy*, **74**(11), 783–795, doi: 10.1007/s001900000142

SMITH W. H. F. & WESSEL P. 1990. Gridding with continuous curvature splines in tension. *Geophysics*, **55**(3), 293-305, doi:10.1190/1.1442837

TAKIN M. & TALWANI M. 1966. Rapid computation of the gravitational attraction of the topography on a spherical Earth. *Geophysical Prospecting*, **14**(), 119-142, doi:

TALWANI M. 1998. Errors in the total Bouguer reduction. *Geophysics*, **63**(), 1125–1130doi:

VANÍČEK P., NOVAK P. & MARTINEC Z. 2001. Geoid, topography, and the Bouguer plate or shell. *Journal of Geodesy*, **75**(4), 210–215, doi: 10.1007/s001900100165

VANÍČEK P., TENZER R., SJÖBERG L. E., MARTINEC Z., FEATHERSTONE W. E. 2004. New views of the spherical Bouguer gravity anomaly. *Geophysical Journal International*, **159**(2), 460-472, doi: 10.1111/j.1365-246X.2004.02435.x.

WATTS, A.B. (2001). *Isostasy and Flexure of the Lithosphere*, Cambridge University Press, Cambridge, UK.

WELLMAN P., MURRAY B. 1985. Australian gravity base station network: BMR Journal of Australian Geology and Geophysics, 9, 225-231 http://www.ga.gov.au/image_cache/GA2235.pdf

WESSEL P. & SMITH W. H. F., 1998. New, improved version of Generic Mapping Tools released. *EOS – Transactions of the American Geophysical Union*, **79**, 579.

Figure 1 Schematic diagram for the spherical terrain corrections

Figure 2 Coverage of the 1,095,065 Australian land gravity observations in the 2007 release from Geoscience Australia (Lambert projection)

Figure 3 The 9-arc-sec by 9-arc-sec (~ 250 m by 250 m) GEODATA (version 2.1) DEM (Hutchinson 2001) (Units in metre, Lambert projection)

Figure 4 Left: simple planar Bouguer gravity anomaly (a), planar terrain correction (b) and complete Bouguer gravity anomaly (c). Right: simple spherical Bouguer gravity anomaly (d), spherical terrain correction (e) and complete spherical Bouguer gravity anomaly (f) (Units in mGal; Lambert projection)

Figure 5 Difference between the complete planar and complete spherical Bouguer gravity anomaly (Units in mGal; Lambert projection)

Table 1 Parameters used to compute the second-order free-air correction (Eq. 3) and normal gravity (Eq. 4). Values for the GRS80 reference ellipsoid are taken from Moritz (1980).

Parameter		Value	Source	Unit
k	normal gravity constant	0.001 931 851 353 0.001 931 852 652	GRS80 WGS84	--
e^2	first numerical ecentricity (squared)	0.006 694 380 022 90 0.006 694 379 999 01	GRS80 WGS84	--
a	ellipsoid semi-major axis	6 378 137 6 378 137	GRS80 WGS84	m
γ_e	equatorial normal gravity	9.780 326 7715 9.780 325 339	GRS80 WGS84	ms^{-2}
f	Flattening	1/298.257 222 101 1/298.257 223 563	GRS80 WGS84	--
m	geodetic parameter	0.003 449 786 003 08 0.003 449 786 506 84	GRS80 WGS84	--
G	gravitational constant	$6.674\ 28(67) \times 10^{-11}$	CODATA	$m^3kg^{-1}s^{-2}$

Table 2 DEM resolutions and spatial extensions used for the practical determination of the global spherical terrain corrections. The spatial extensions are given as arc-distances along a parallel and meridian and define an area centred around each computation point.

Resolution	**Extension**	**DEM Source**
9″ x 9″	30′ x 30′	GEODATA
45″ x 45″	2º x 2º	GEODATA/GLOBE
3′ x 3′	4º x 4º	GEODATA/GLOBE
15′ x 15′	10º x 10º	GEODATA/GLOBE/JGPE95E
60′ x 60′	Global	GEODATA/GLOBE/JGPE95E

Table 3 Descriptive statistics of various gravity anomalies and terrain corrections at the 1,095,065 Australian land gravity observation locations, and statistics of the planar and spherical terrain corrections at the gravity observation locations and over the whole 9-arc-second Australian grid (units in mGal)

Data type	Min.	Max.	Mean	Stdv.	RMS
Fee-air gravity anomalies	-112.32	172.79	5.56	±24.96	±25.602
Planar Bouguer gravity anomalies					
Simple	-163.79	83.09	-20.59	±29.13	±35.67
Complete	-163.74	83.09	-20.38	±29.13	±35.55
Planar terrain corrections					
At location of gravity stations	0.00	30.10	0.20	±0.79	±0.82
9-arc-sec grid	0.00	53.71	0.08	±0.48	±0.48
Spherical Bouguer gravity anomalies					
Simple	-285.90	83.09	-46.85	±43.83	±64.16
Complete	-184.00	65.36	-39.04	±29.66	±49.03
Spherical terrain corrections					
At location of gravity stations	-20.10	229.12	7.80	±20.40	±21.84
9-arc-sec grid	-19.44	257.65	11.74	±21.33	±24.35

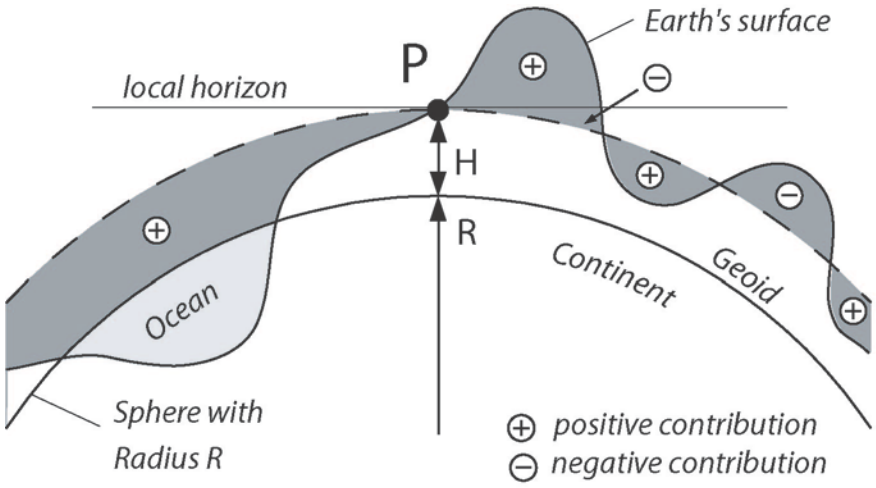

Figure 1 Schematic diagram for the spherical terrain corrections

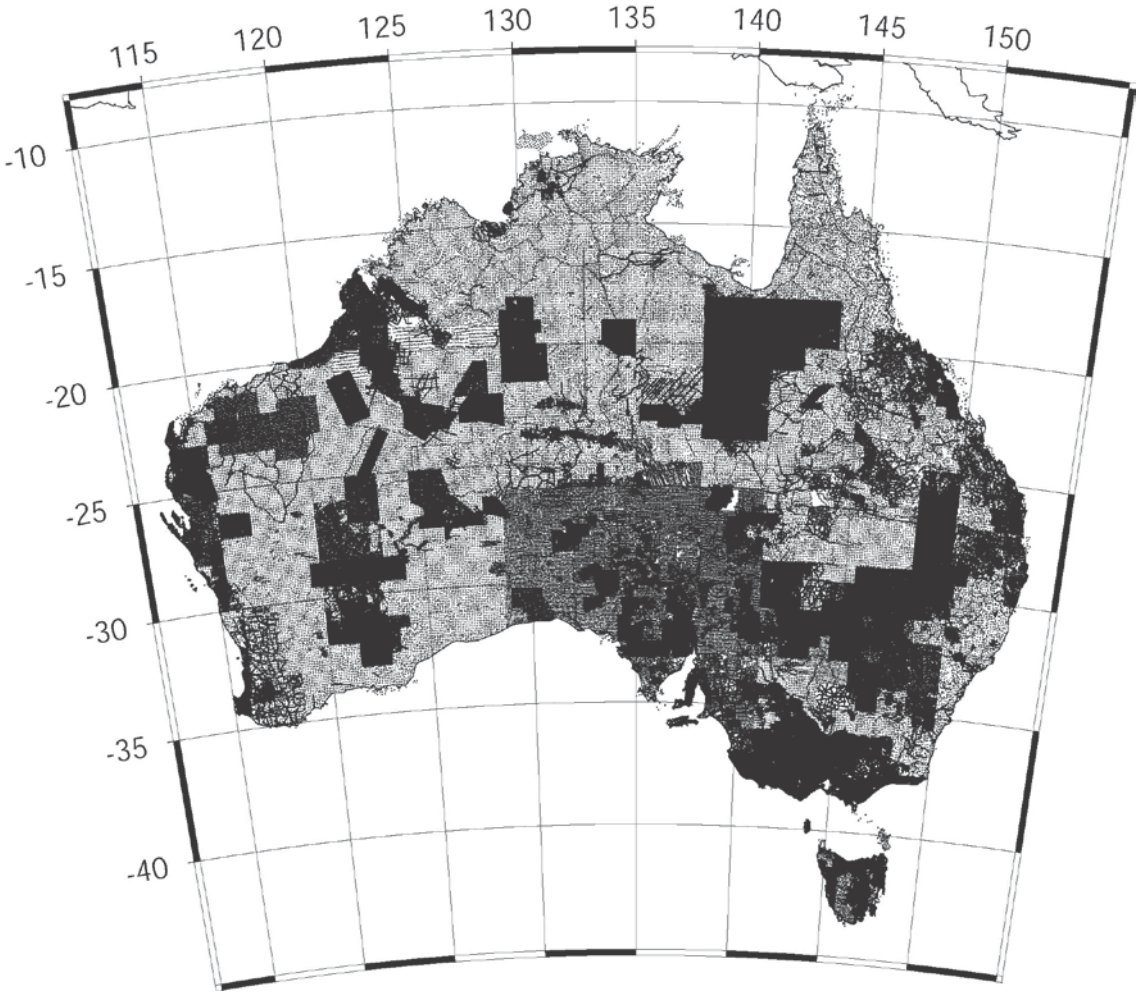

Figure 2 Coverage of the 1,095,065 Australian land gravity observations in the 2007 release from Geoscience Australia (Lambert projection)

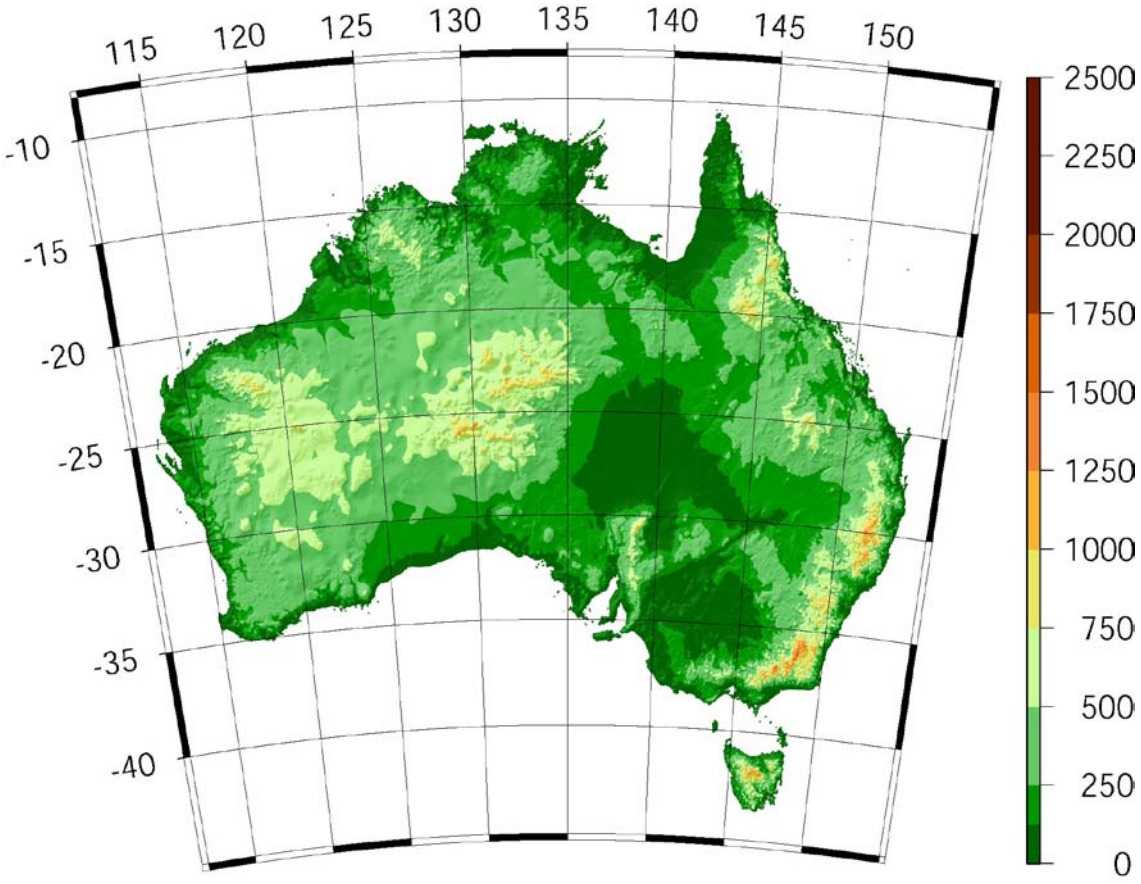

Figure 3 The 9-arc-sec by 9-arc-sec (~ 250 m by 250 m) GEODATA (version 2.1) DEM (Hutchinson 2001). (Units in metre, Lambert projection)

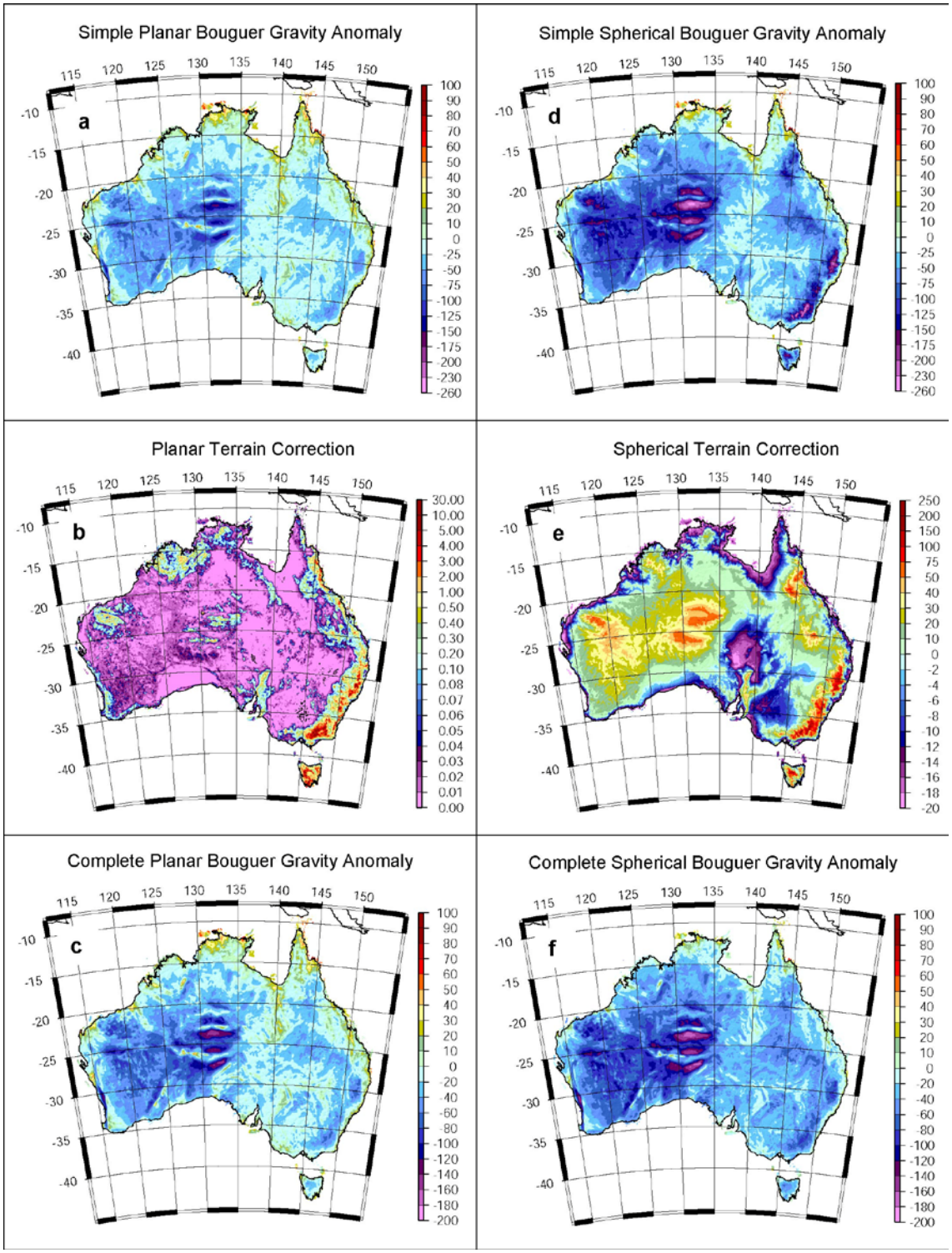

Figure 4 Left: simple planar Bouguer gravity anomaly (a), planar terrain correction (b) and complete Bouguer gravity anomaly (c). Right: simple spherical Bouguer gravity anomaly (d), spherical terrain correction (e) and complete spherical Bouguer gravity anomaly (f) (Units in mGal; Lambert projection)

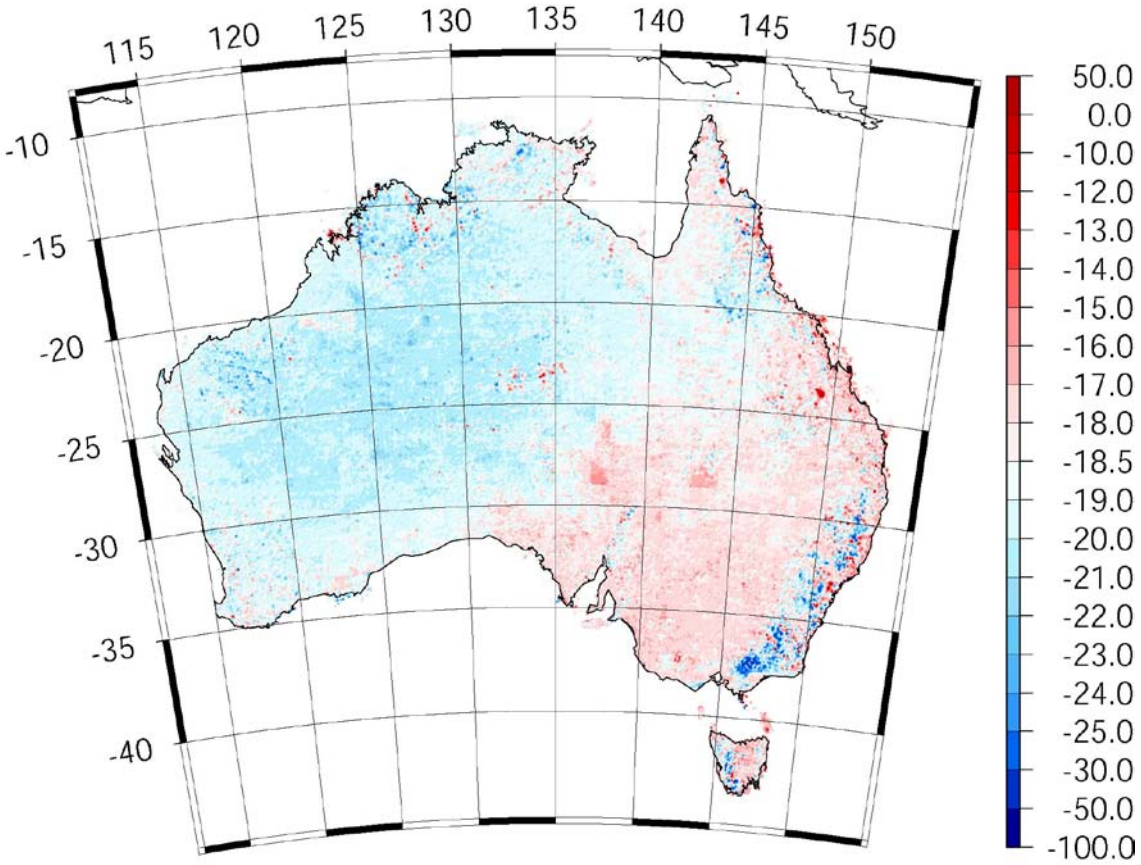

Figure 5 Difference between the complete planar and complete spherical Bouguer gravity anomaly (Units in mGal; Lambert projection)